ОБЪЕДИНЕННЫЙ
ИНСТИТУТ
ЯДЕРНЫХ
ИССЛЕДОВАНИЙ
Дубна

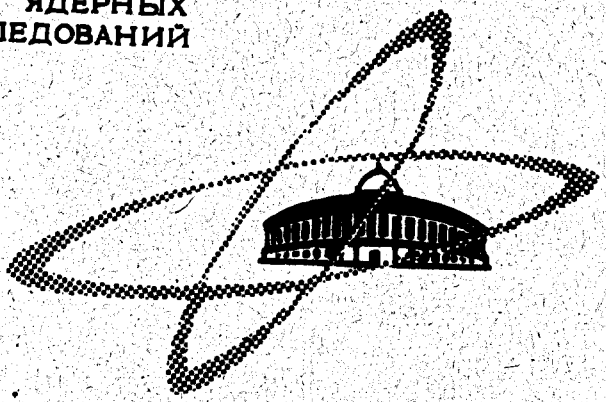

E2 - 4607

V.S.Barashenkov, K.K.Gudima, S.M.Eliseev,
A.S.Iljinov, V.D.Toneev

INELASTIC INTERACTIONS OF PIONS AND NUCLEONS WITH NUCLEI AT HIGH AND SUPERHIGH ENERGIES (INTRANUCLEAR CASCADES, MULTIPLE-PARTICLE INTERACTIONS)

ЛАБОРАТОРИЯ ТЕОРЕТИЧЕСКОЙ ФИЗИКИ

1969

E2 - 4607

V.S.Barashenkov, K.K.Gudima, S.M.Eliseev,
A.S.Iljinov, V.D.Toneev

INELASTIC INTERACTIONS OF PIONS AND NUCLEONS WITH NUCLEI AT HIGH AND SUPERHIGH ENERGIES (INTRANUCLEAR CASCADES, MULTIPLE-PARTICLE INTERACTIONS)

(Report submitted to the III International Conference on High Energy Physics and Nuclear Structure, New York, 1969).

1. Detailed calculations showed that the inelastic pion- and nucleon -nucleus interactions are well accounted for by the mechanism of intranuclear cascades in the whole range of the primary particle energies T from a few dozens of MeV to a few GeV. Some examples illustrating the agreement between theory and experiment in this energy range are given in Figs. 1,2 and in Table I.

Good agreement of the cascade calculations with experiment is obtained not only for interactions of elementary particles with nuclei but also for interactions of deuterons with nuclei (see e.g. Fig.3).

Discrepancies with experiment at $T \lesssim 1$ GeV indicated in some papers are due to shortcomings of particular versions of the cascade models rather than to the violation of the cascade mechanism itself [1].

However, attempts to extend directly the intranuclear cascade model to the energy range $T > 10$ GeV lead immediately to an essential disagreement with experiment which increases with increasing T.

Our aim is to consider at what energies the usual cascade mechanism changes, and in what characteristics these changes are revealed most strongly. We would like aslo to discuss the causes of such changes.

2. One of the most serious difficulties encountered in calculating the intranuclear cascades is the necessity to introduce detailed information on inelastic particle interactions at different energies into the computer. This imposes high requirements to the computer area storage and in many case, especially in the energy range when the multiple-particle production is of importance , turns out to be completely impossible owing to the absence of necessary experimental data.

The calculation becomes essentially simpler when as the initial information for the simulation of the picture of an elementary act one uses instead of the elementary distributions their polynomial approximations. To find such approximations a laborious numerical analysis of a large number of experimental data is needed. However, the approximations obtained in such a way can be used in calculating the cascades in various nuclei and at various energies.

It should be noted that the energy dependence of the characteristics of elementary interactions turns out to be in this case continuous which considerably improves the accuracy of calculations.

It order to obtain the approximation mentioned one should use instead of the differential angular and momentum distributions in the c.m.s $\omega_\theta(\cos\theta)$ and $\omega_p(p)$ the corresponding integral distributions

$$W_\theta(x)=\int_0^x \omega_\theta(2z-1)\,dz \Big/ \int_0^1 \omega_\theta(2z-1)\,dz\,,\quad W_p(y)=\int_0^y \omega_p(p_{max}\cdot z)\,dz \Big/ \int_0^1 \omega_p(p_{max}\cdot z)\,dz.$$

and bear in mind that the inverse quantities

$$x = W_\theta^{-1}(\xi) \quad \text{and} \quad y = W_p^{-1}(\xi)$$

are monotonously increasing functions of a random number ξ uniformly distributed over the interval $[0,1]$. These functions expressed in terms of the polynomials in ξ read:

$$\cos\theta = 2\xi^{1/2}\{\sum_{n=0}^{N} a_n \xi^n + (1-\sum_{n=0}^{N} a_n)\,\xi^{N+1}\} - 1,$$

$$p = p_{max}\xi^{1/2}\{\sum_{n=0}^{N} b_n \xi^n + (1-\sum_{n=0}^{N} a_n)\,\xi^{N+1}\},$$

where the maximum momentum p_{max} in the experimental distribution and the coefficients a_n and b_n depend on the type of the reaction considered and on the colliding particle energy. The energy dependence of these quantities can also be represented in the polynomial form

$$a_n = \sum_{k=0}^{M} a_{nk} T^k , \qquad b_n = \sum_{k=0}^{M} b_{nk} T^k , \qquad p_{max} = \sum_{k=0}^{M} c_k T^k .$$

The detailed calculations showed that within the accuracy of the present-day experiments the approximation by the polynomials of fourth degree (i.e. $N=3$, $M=3$) appears to be optimum. Such polynomials are simple for calculations and at the same time well approximate the available experimental data (see, for example, Figs. 4 and 5).

The tables of the coefficients a_{nk}, b_{nk} and c_k are given in ref.[2b].

The polynomial approximation can be used not only for inelastic channels but also for the angular distribution of elastically scattered particles (the particle energy is unambiguously defined by the scattering angle).

Another fact which essentially influences the accuracy of cascade calculations is the necessity for the energy and momentum conservation laws to be satisfied when each act of inelastic $\pi - N$ or $N-N$ interaction is simulated by the Monte-Carlo method. In order to calculate the integral average quantities like the average multiplicity and the average energy of secondaries it is sufficient to take into account these laws only statistically, i.e. on the average over a large number of interactions[3-5]. In so doing one obtains quite good results also for the total angular and energy distributions.

Fig.6 shows the distribution of the difference of the total particle energies before and after interaction, ΔE, for various kinds and energies of projectiles. The mean value of ΔE does not practically differ from zero however the dispersion turns out to be surprisingly large and the "tail" of the distribution goes up to $\Delta E = T$[6]. This may lead to noticeable errors in characteristics such as the number of

particles in a fixed energy interval, the particle spectrum at a fixed angle and so on. The excitation energy of the residue nucleus and, consequently, the number of black prongs in the star are found to be especially vulnerable.

A rather effective method of simulating the inelastic elementary particle interactions with exact account of the energy and momentum conservation laws has recently been developed in our laboratory (the histograms in Figs. 4 and 5 were obtained by just this method).

3. From Fig.7 it is seen that the theoretical average multiplicities $\bar{n}_g$ and $\bar{n}_h$ in proton-nucleus collisions which are in good agreement with experiment at $T < 5$ GeV do not reflect the experimentally observed "saturation" at higher energies. The calculated $\bar{n}_s$ values are very close to the experimental ones up to $T \cong 20$ GeV where there appear noticeable disagreements.

Similar results were obtained for pion-nuclear interactions. But here it is difficult to speak of the difference between theoretical and experimental $\bar{n}_s$ values since the measurements are performed as yet only at $T < 20$ GeV.

The difference between theoretical and experimental characteristics is revealed more clearly in considering the particle correlations. It is seen from Fig.8 that at $T < 5$ GeV the dependence of $\bar{n}_s$ on the number of h -prongs in the star is in good agreement with experiment while at higher energies the calculated histograms differ noticeably from the measured ones.

As to the dependence of the average number of grey tracks on the number of s-particles, at $T \gtrsim 5$ GeV it is impossible to speak of even qualitative agreement with experiment (Fig.9). At less higher energies there are no direct measurements however the character of the correlations at $T = 3.2$ GeV in proton-nuclear interactions is about the same as in π^- -meson -nucleus collisions at $T = 1.87$ GeV, where one observes a decrease of the average number of g -prongs with increasing n_s /7/.

The analysis of the energy characteristics of secondaries showed that the disagreement between the calculated and experimental

average multiplicities is accompanied by a softening of the energy spectrum of g-particles (Fig.10) although the s-particle spectra are reproduced quite satisfactory.

It should be noted that the deflection of the energy and especially of the angular characteristics from the experimentally observed ones is noticeably smaller than for the multiplicity. For example, the difference of the experimental and theoretical $\bar{n}_g$ by more than a factor of two in proton-nuclear interactions at $T = 22.5$ GeV is accompanied by only a 5% discrepancy in the average g-particle energies. The difference in the angular particle distributions is found to be even smaller.

The experimentally observed "saturation" of the number of g- and h-particles which may be considered as the "saturation" of the number of recoil nucleons and the excitations energy of the residue-nucleus allows one to explain qualitatively also some other important facts concerning fragmentation, spallation and fission of nuclei.

If the fragments are assumed to be nucleon associations knocked out of the nucleus by cascade nucleons or produced by evaporating from a excited residue-nucleus then the increase of their production cross sections slows down at $T \approx 5$ GeV (for the average emulsion nucleus). This has been observed in experiment.

Next, since the h-particles carry away the main part of the mass lost by the target-nucleus then the parameters charaterising the mass distribution as a function of energy T must also tend to the "saturation" at energies of the order of a few GeV. The analysis of the radiochemical measurements for nuclei in the middle of the Mendeleev Table confirms this conclusion[8].

At energies higher than several hundreds of MeV, with further increasing T, the growth of the excitation energy compensates only partially the increase of the fission barrier which is due to still deeper spallation of nuclei. This leads to a decrease of the fission cross section σ_f with increasing T. However at energies

of the order of a few GeV and higher this decrease must slow down. The results of recent measurements confirm this conclusion too[9].

None of the effects just mentioned is explained by the usual cascade model.

At energies $T \gtrsim 100$ GeV the difference between the cascade calculations and experiment becomes over more essential. For example, at $T \cong 10^3$ GeV the theoretical s -particle multiplicity is larger than the experimental one by about a factor of three; some disagreement is observed in the angular distributions too[4].

4. Thus, the deflections from the ordinary cascade theory start to reveal first of all in the characteristics of the low-energy component of produced particles at $T \gtrsim 5$ GeV. The estimates show that there are several reasons for such deflections. First, in all cascade calculations yet performed one ignores completely the fact that, as the cascade develops, a still larger number of intranuclear nucleons is involved in it, owing to which the low-energy component of cascade particles meets on its way smaller nuclear density. The number of "evaporation" particles decrease, as well.

Another important fact which is disregarded in cascade calculations consists in that at energies higher than a few GeV resonons are intensively produced in $\pi - N$ and $N - N$ collisions which are then involved in the intranuclear cascade. From the kinetical point of view this is to some extent equivalent to the simultaneous interaction of several "stuck together" particles with an intranuclear nucleon.

With further increasing energy T, owing to relativistic contraction the angles of emission of particles produced in $\pi - N$ and $N - N$ -collisions become so small that any discrimination of the times of interactions of these particles with an intranuclear nucleon is meaningless. In other words, there occurs simultaneous scattering and absorption of several particles on one nucleon (the absorption of a resonon by a nucleon may be considered as a particular case of such multiple -particle interactions). Since at present we know nothing about the properties of multiple -particle interactions (MPI)

it is advisable to consider the inverse problem: let us attempt to obtain some information on these interactions from the analysis of the experimental data of cosmic-ray experiments. We should begin the calculation , of course, from the most general assumptions on the character of MPI and then should introduce further details only as far as it becomes quite necessary for obtaining agreement between the calculation results and experiment. Such an approach would guarantee against the introduction to the theory of unjustified assumptions.

The location of intranuclear nucleons was sampled by the Monte-Carlo method for each interaction of a primary with the nucleus; this location was considered to be unchanged during the time of cascade development. It was assumed that all the particles the free paths of which end near the center of the intranuclear nucleon at distances shorter than its radius interact simultaneously with this nucleon. The properties of such MPI were supposed to be dependent on only the value of the "free" energy $\epsilon = \sqrt{(\Sigma E_i)^2 - (\Sigma \vec{p}_i)^2} - \Sigma M_i$ which can be spent for the production of new particles (E_i , $\vec{p}_i$, M_i are the total energy, momentum and mass of the i -th particle absorbed by a nucleon). In inelastic $\pi - N$ and $N-N$ collisions the energy and momentum conservation laws were taken into account only statistically.

It is clear that such a model gives a rather simplified description of the physical process. However even in this case one can draw a number of quite definite and rather general conclusions.

It is seen from Fig.11 that even at $T \cong 10$ GeV the number of MPI in the average emulsion nucleus is about 20% and at $T \approx 10^3$ it reaches 40%. In this case the fraction of particles involved in MPI increases from 30 to 70%.

It should be however noted that the large contribution of MPI at $T \cong 10$ GeV appears to be due to the fact that in calculations the decrease of the nuclear density was disregarded and all the deflections from the usual cascade model were ascribed to the MPI effect. The account of the decrease in the number of intranuclear nucleons is a very complicated problem which we have just began to solve.

With the aid of computers we have performed several series of calculations which differ by the assumptions on the MPI properties. One succeeds in obtaining agreement with experimental data over the range $T \approx 30 - 10^3$ GeV only if the angular and energy distributions of particles produced in MPI are chosen in the form given in Figs. 13 and 12 and besides the existence of a leading particle carrying away 50-70% of the total energy is assumed.

Of course, the details in the distributions in Figs. 12 and 13 may be considered for the time being only qualitatively. However, the fact itself of the existence of MPI and the fact that the characteristics of particles produced in such interactions are close to those observed in ordinary two-particle interactions at high energies (in particular, the presence of the leading particle and the asymmetry character of the angular distributions of the remaining particles) may be considered to be rather reliable.

Table II and Fig.14 show good agreement between the calculation results taking intc account MPI and experiment.

In conclusion we would like to stress once more that the study of the particle- nucleus interaction mechanism at high and superhigh energies depends essentially on the "transition" energy region $T = 2 - 30$ GeV. It is interesting to study not so much integral, average characteristics as the differential distributions and correlations between various quantities. Particular attention should be given to the low-energy component of produced particles.

References

1. *V.S.Barashenkov, K.K.Gudima, V.D.Toneev. JINR Preprints, P2-4302, P2-4313, P2-4346, P2-4402, Dubna (1969).*
2. *V.S.Barashenkov, K.K.Gudima, V.D.Toneev. JINR Preprints, P2-4065, P2-4066, Dubna (1968).*
3. *I.Z.Artykov, V.S.Barashenkov, S.M.Eliseev. Yader. Fizika, 4, 156 (1968).*

4. I.Z.Artykov, V.S.Barashenkov, S.M.Eliseev. Nucl. Phys., 87, 241 (1966).
5. I.Z.Artykov, V.S.Barashenkov, S.M.Eliseev. Nucl. Phys., B6, 11 (1968); B6, 628 (1968).
6. N.M.Sobolevski, V.D.Toneev. Acta Phys.Polon., 35, 367 (1969).
7. VB.E.Ronne, O.Danielson. Arkiv for Phys., 22, 175 (1962).
8. G.Rudstam. Z. Naturforsch, 21a, 1027 (1966).
9. E.S.Matusevich, V.N.Regushevski. Yader. Fizika, 7, 1187 (1968).

Received by Publishing Department
on July 16, 1969.

Table 1

Fraction of protons of energy T_p higher than 30 and 100 MeV (in %) in stars with different number of of black progns n_b . Energy of primary protons T= 385 MeV

	$T_p > 30$ MeV		$T_p > 100$ MeV	
n_g	Theory	Experiment	Theory	Experiment
0	98 ± 6	-	82 ± 7	-
1	86 ± 5	81 ± 13	62 ± 6	58 ± 12
2	80 ± 5	77 ± 13	49 ± 3	49 ± 8
3	71 ± 4	66 ± 12	41 ± 3	40 ± 8
4	80 ± 6	61 ± 12	40 ± 5	24 ± 7
5	40 ± 6	52 ± 12	12 ± 8	19 ± 7
6	45 ± 8	23 ± 2	0	12 ± 11
7	0	7 ± 7	0	0

Table II

Comparison of the results of cascade calculations taking into account multiple particle interactions with experiment

T, GeV	Interaction	Characteristics	Theory	Experiment x
100	p+LEm	$\bar{n}_s$	7.9±0.4	7.4±0.5
		$\bar{T}_s$, GeV	3.1±0.2	2.9±0.3
	p+Em	$\bar{n}_s$	10.3±0.5	8.0±0.5
		$\bar{n}_g$	3.6±0.2	5.0±1.6
		$\bar{T}_s$, GeV	2.8±0.2	2.4±0.9
200	π^-+LEm	$\bar{n}_s$	9.7±0.4	8.0±0.9
		$\theta_{1/2s}$°	6.5±0.3	6.2±0.4
	π^-+Em	$\bar{n}_s$	11.2±0.6	10.8±0.9
		$\theta_{1/2s}$°	9.0±0.5	8.3±0.6
	π^-+HEm	$\bar{n}_s$	15.4±0.7	14.7± 2.0
		$\theta_{1/2s}$°	12.0±0.6	11.0±1.1
500	p+Em	$\bar{n}_s$	18.0±0.9	18.8±4.2
		$\bar{n}_g$	3.7±0.2	4.0±0.8
10^3	p+LEm	$\bar{n}_s$	12.1±0.6	9.9±1.4
	p+Em	$\bar{n}_s$	20.5±1.1	22.5±3.0
		$\bar{n}_g$	3.6±0.2	4 ±1.6

x/ For references see paper [5].

LEm, Em, HEm – are medium and medium-heavy emulsion nuclei respectively; $\bar{T}_s$ is the mean energy of secondaries (except the leading one); $\theta_{1/2s}$ is the angle within which half of the s-particles are emitted (lab. system).

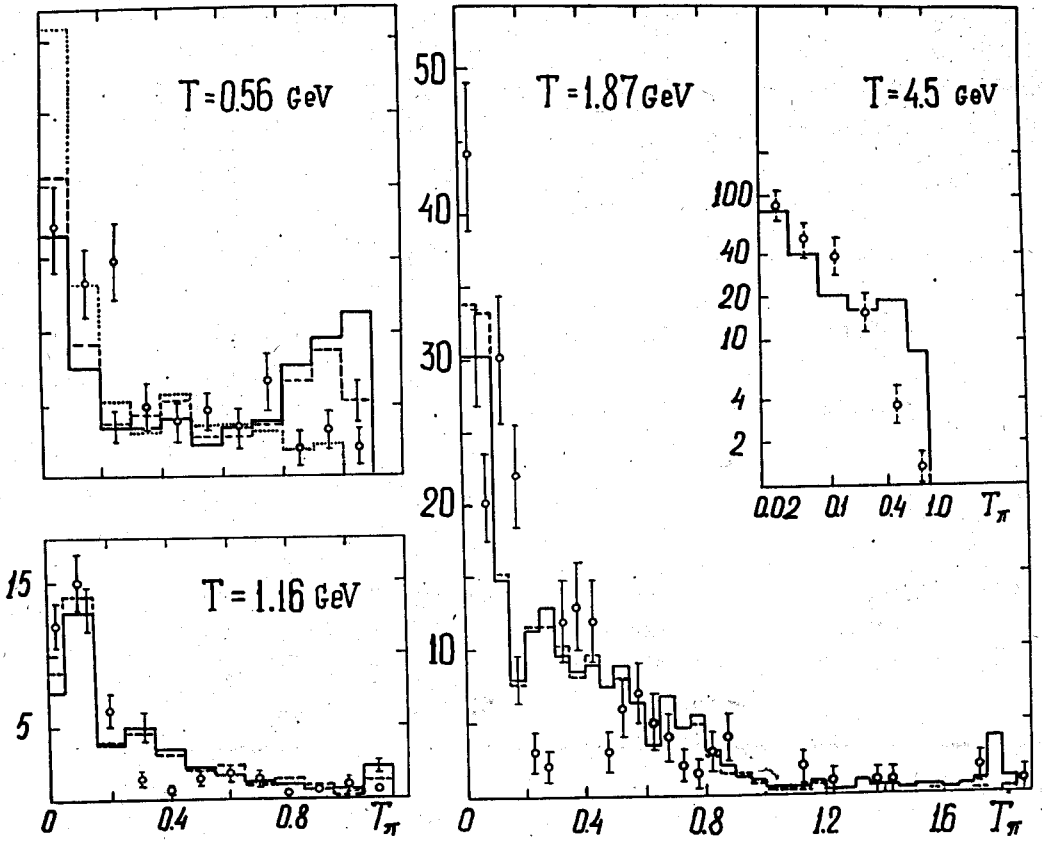

Fig.1. Energy spectra of $\pi^{\pm}$-mesons produced in the collision of π^--mesons of energy T with the emulsion nuclei. (In arbitrary units, the energy T_π in GeV). Continuous, dashed and dotted histograms are the calculation results for stars with $n_h \geq 0$, $n_h \geq 1$ and $n_h \geq 2$ respectively.

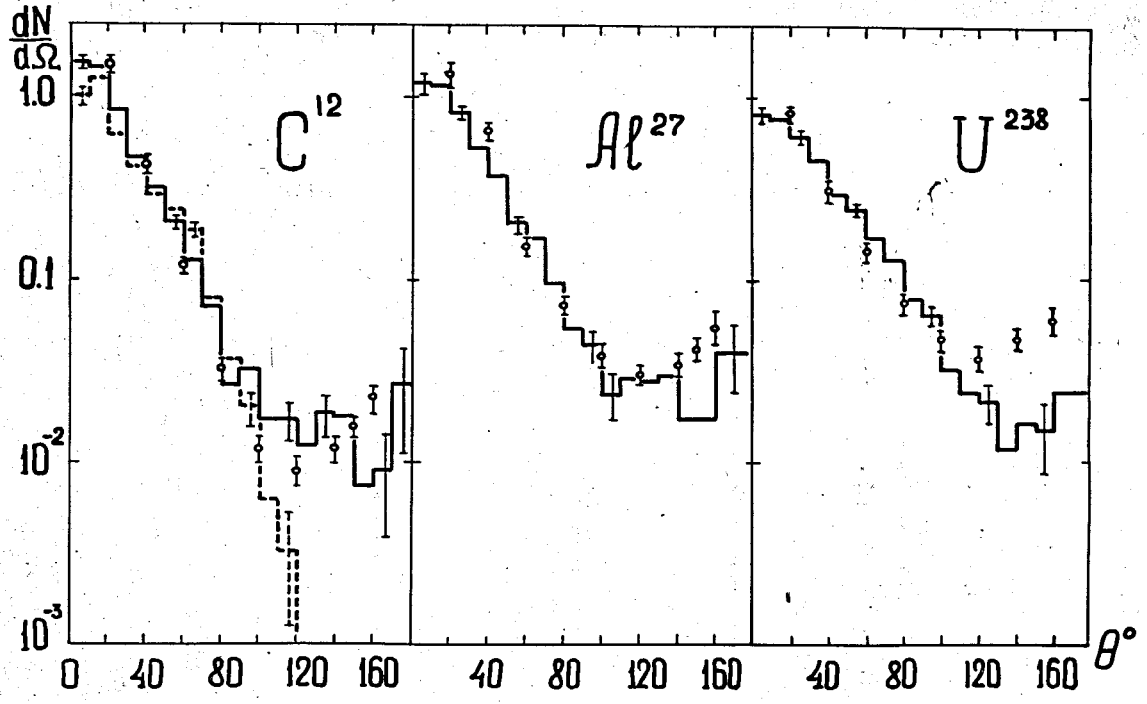

Fig.2. Angular distributions of nucleons with an energy $T_N > 60$ MeV produced in the interaction of 660 MeV protons with different nuclei. The histograms are the calculation results; the dashed line is the calculation result for ^{12}C without the account of inelastic N–N interactions inside the nucleus.

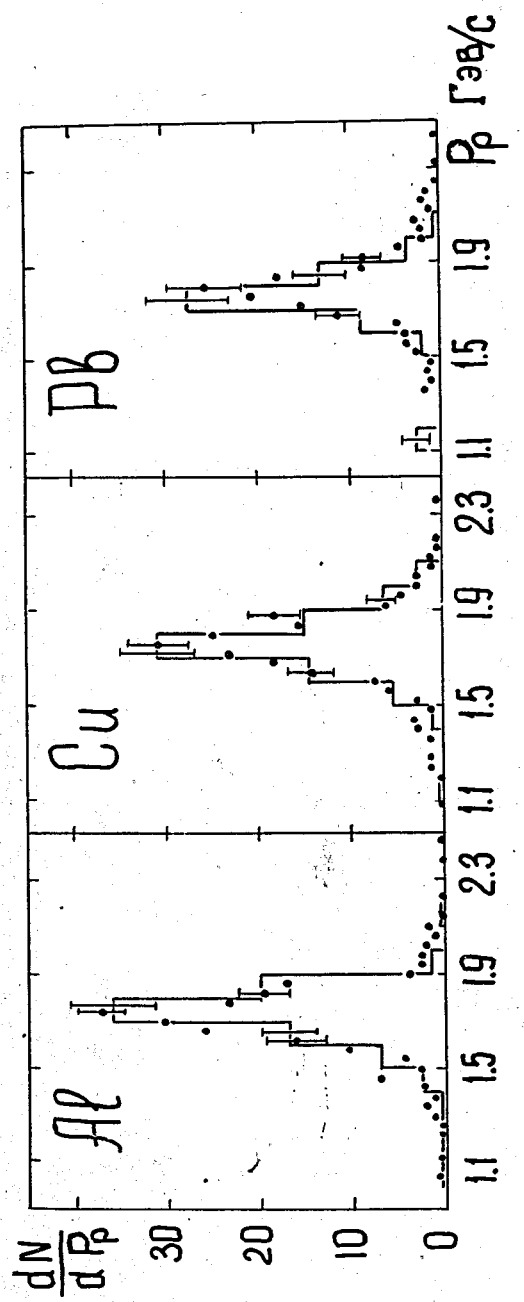

Fig.3.Momentum distributions of protons produced in inelastic collisions of deuterons with nuclei at T = 2.1 GeV. The histograms are the calculation by the cascade model.

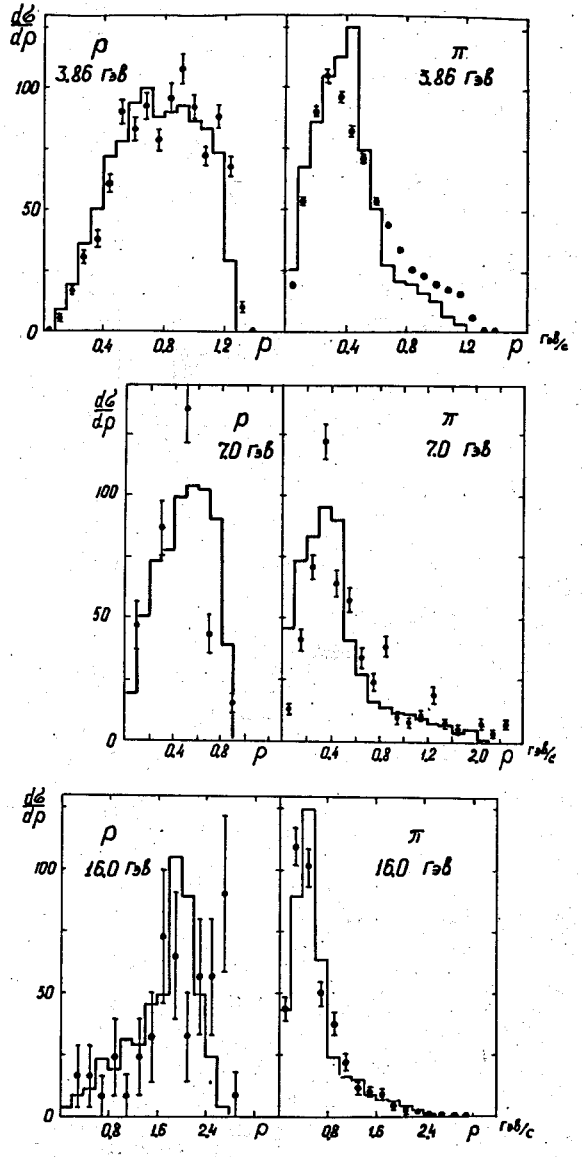

Fig.4.Momentum distributions of protons and pions in the reactions $\pi^- + p \to N + n\pi$, $n > 2$. The energy of the primary π^--mes T is measured in GeV. The histograms are the calculation results by the Monte-Carlo method with the use of the polyno approximation.

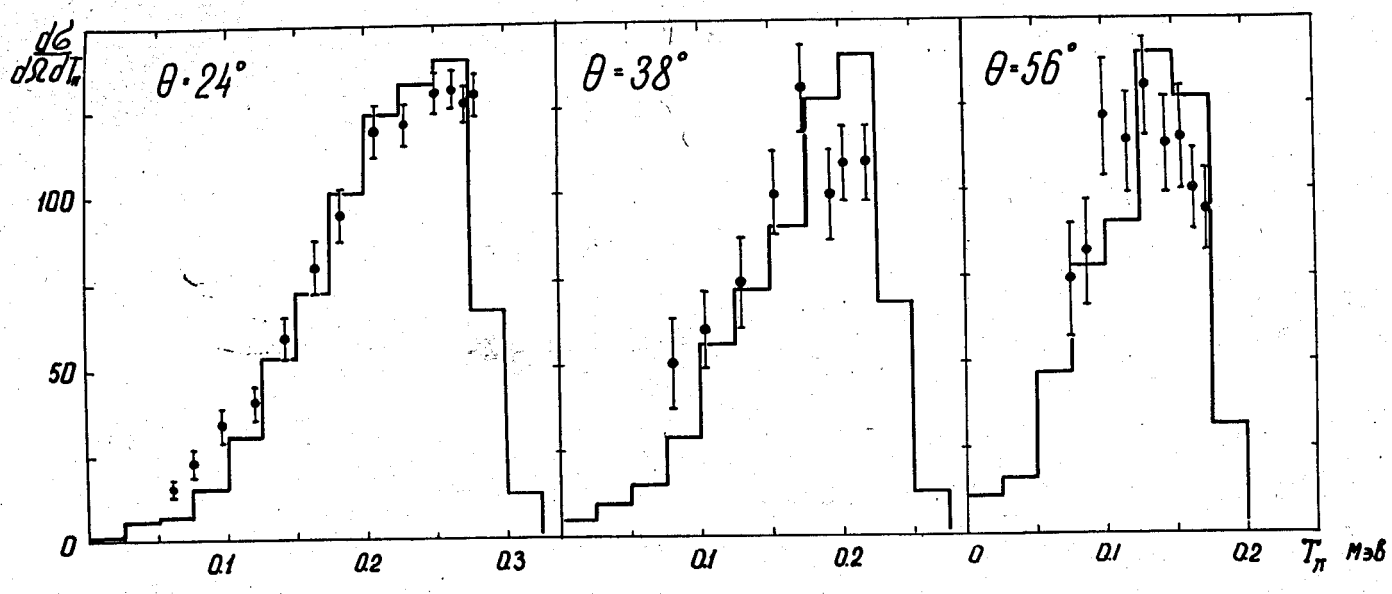

Fig.5. Energy spectra of $\pi^{\pm}$-mesons at an angle θ in the reaction $p+p \to 2N+\pi$ at T = 670 MeV. The histograms are the calculation results obtained by the Monte-Carlo method with the use of the polynomial approximation.

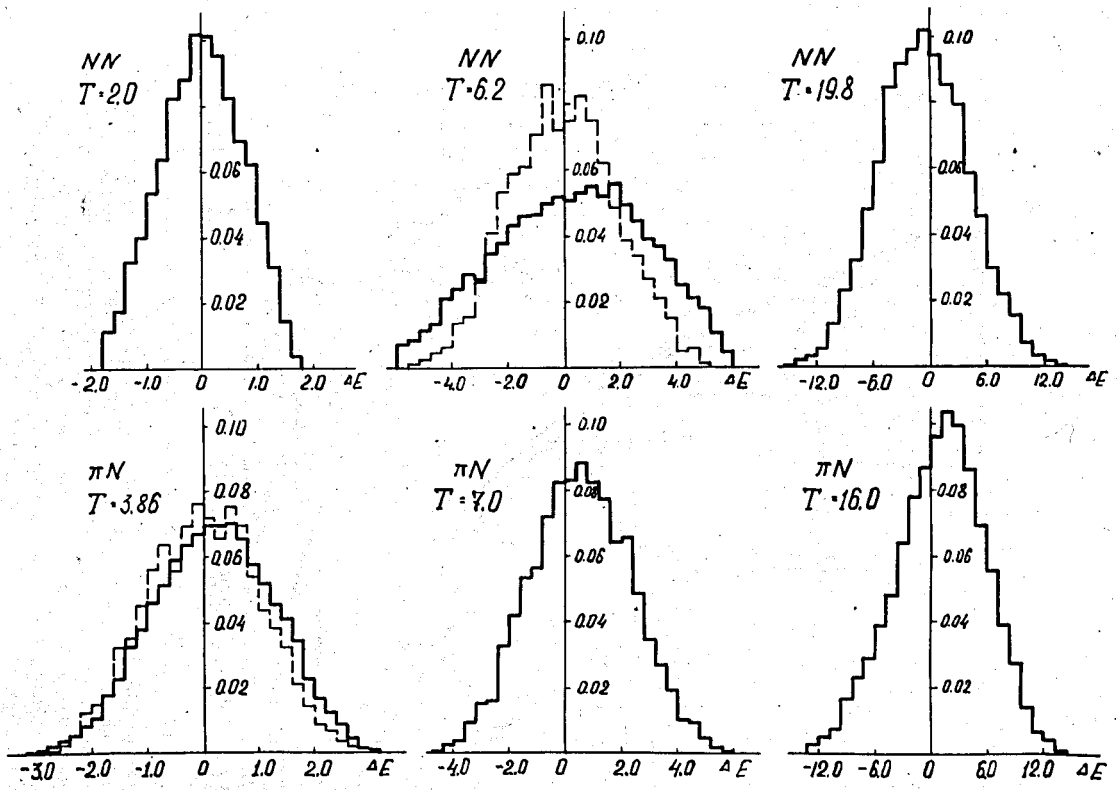

Fig.6. Distribution of the energy difference ΔE (in GeV, in the lab. system) for π- N and N-N interactions at an energy T (in GeV). The dashed line is the distributions calculated under the simpli-

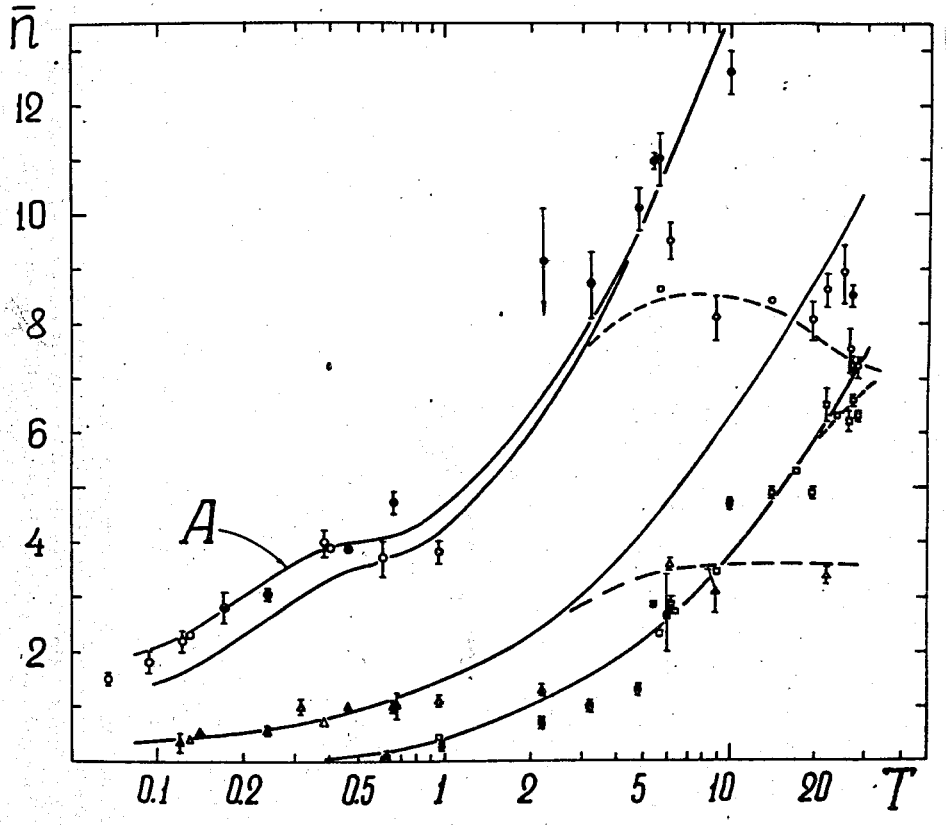

Fig.7. Dependence of the average number of s-, g- and h-particles in emulsion stars on the primary proton energy . The continuous lines are the calculation results for all stars; the curve A is the calculated $\bar{n}_h$ (T) for stars with $n_h > 1$. The dashed lines approximate most reliable experimental points. The marks O, Δ and □ are the experimental values of $\bar{n}_h$, $\bar{n}_g$ and $\bar{n}_s$ respectively obtained by scanning "along track". The shaded marks are related to the values obtained by area scanning method.

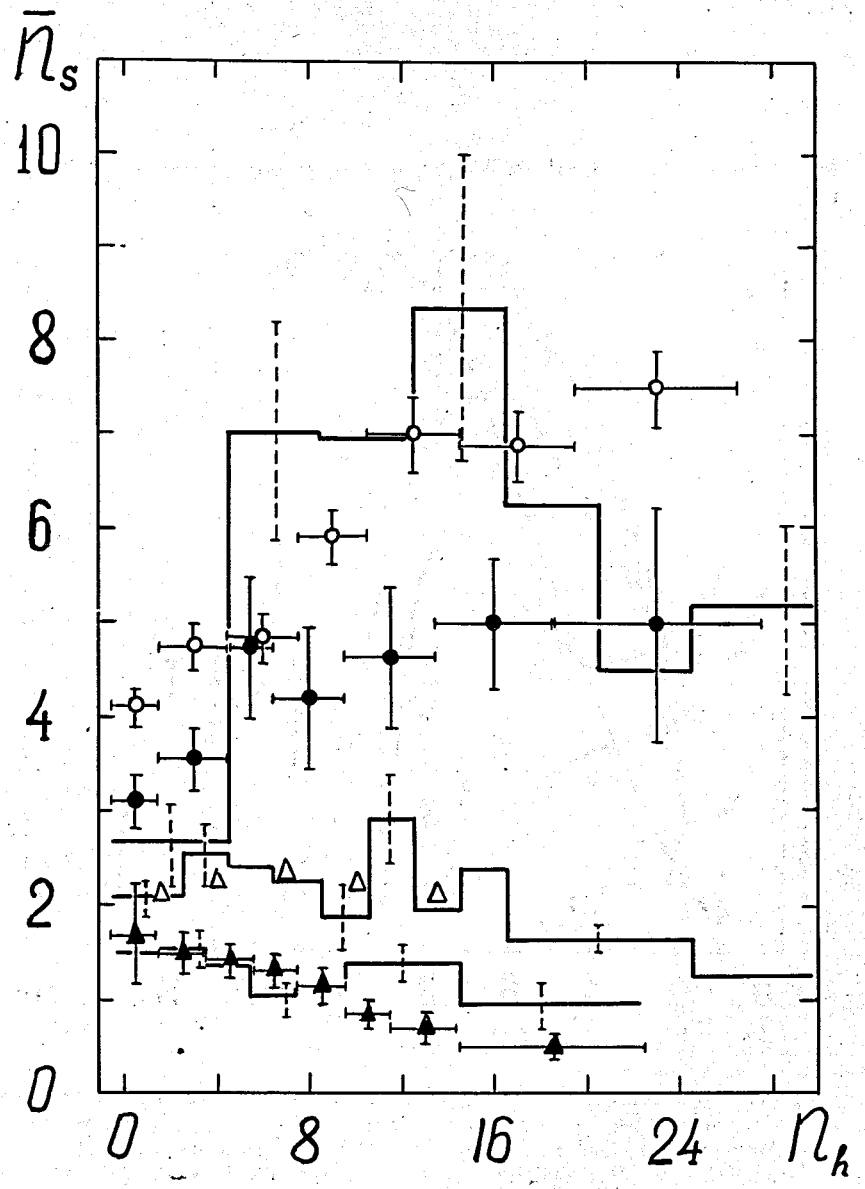

Fig.8. Correlation of the average number of s-tracks and of the number of h-tracks in emulsion stars produced by π^- sons. The marks ▲, Δ, ● and O show the experimental data for T = 1.87, 4.2, 10 and 16.1 GeV respectively. histograms are the calculation results for T = 1.87, 4.2 a 16.1 GeV.

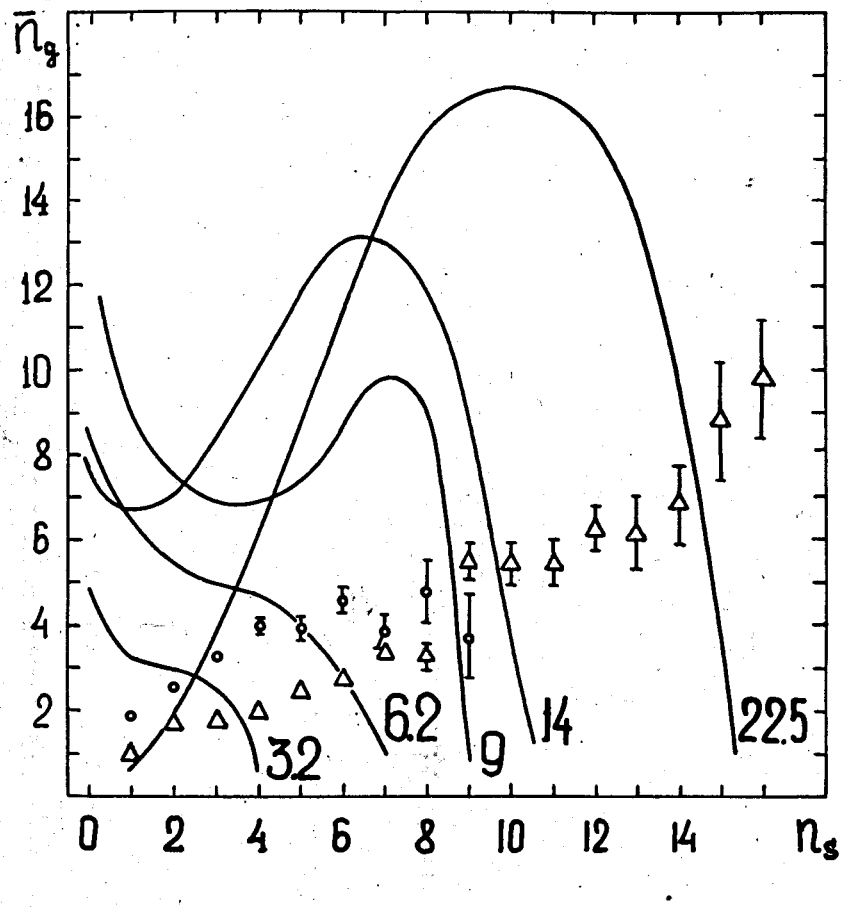

Fig.9. Average multiplicity of g -tracks as a function of the number of ^{s} -particles in emulsion stars produced by protons, the curves are the calculation results; the numbers near the curves are the primary proton energy in GeV. The circles and triangles give the Winzeler's experimental data for T = 6.2 and 22.5 GeV.

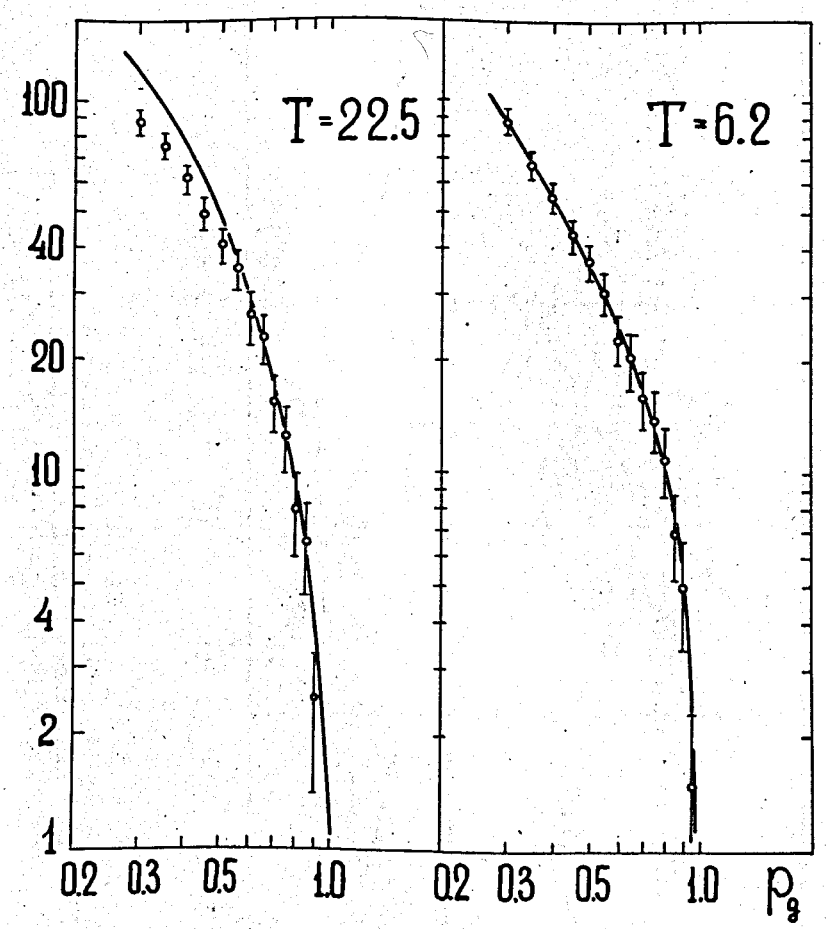

Fig.10. Energy spectra of g -particles $N(\geq p) = \int_{p}^{p_{max}} \omega(p)\,dp$ from proton-nucleus collisions at an energy T . The curves are the calculation results by the cascade theory.

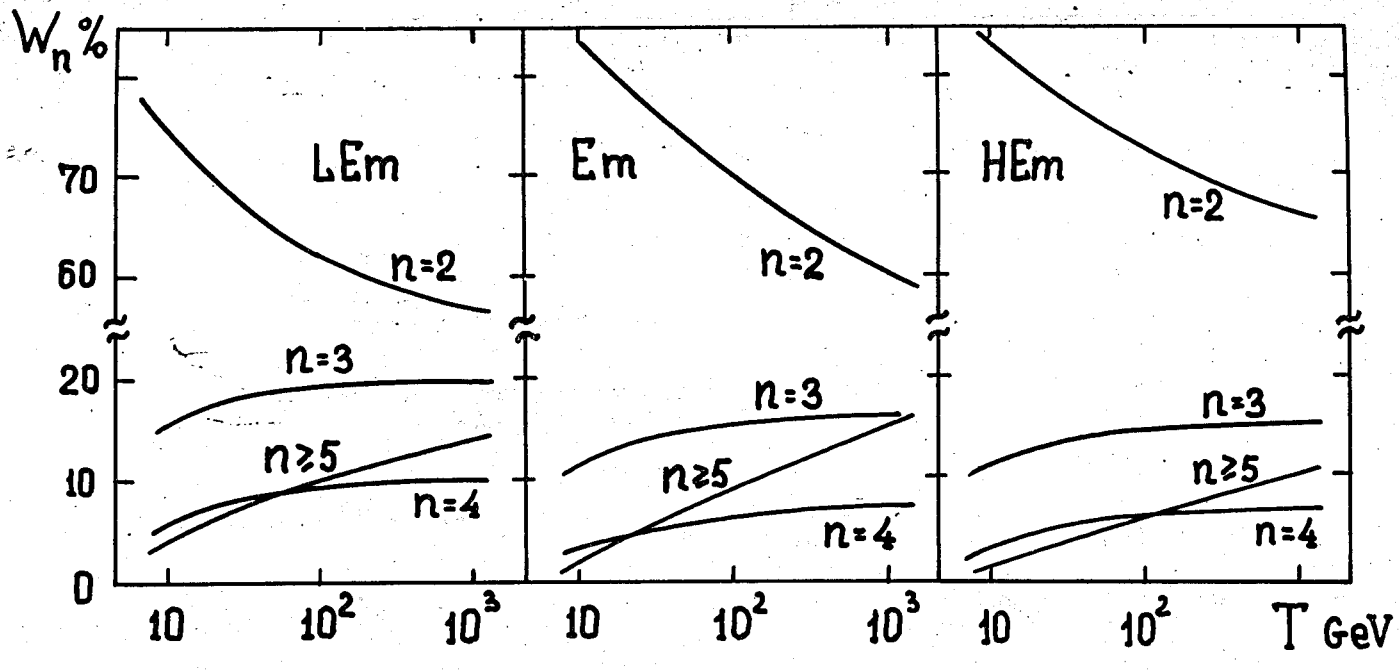

Fig.11. Relative number of intranuclear collisions with n particles in the initial state.

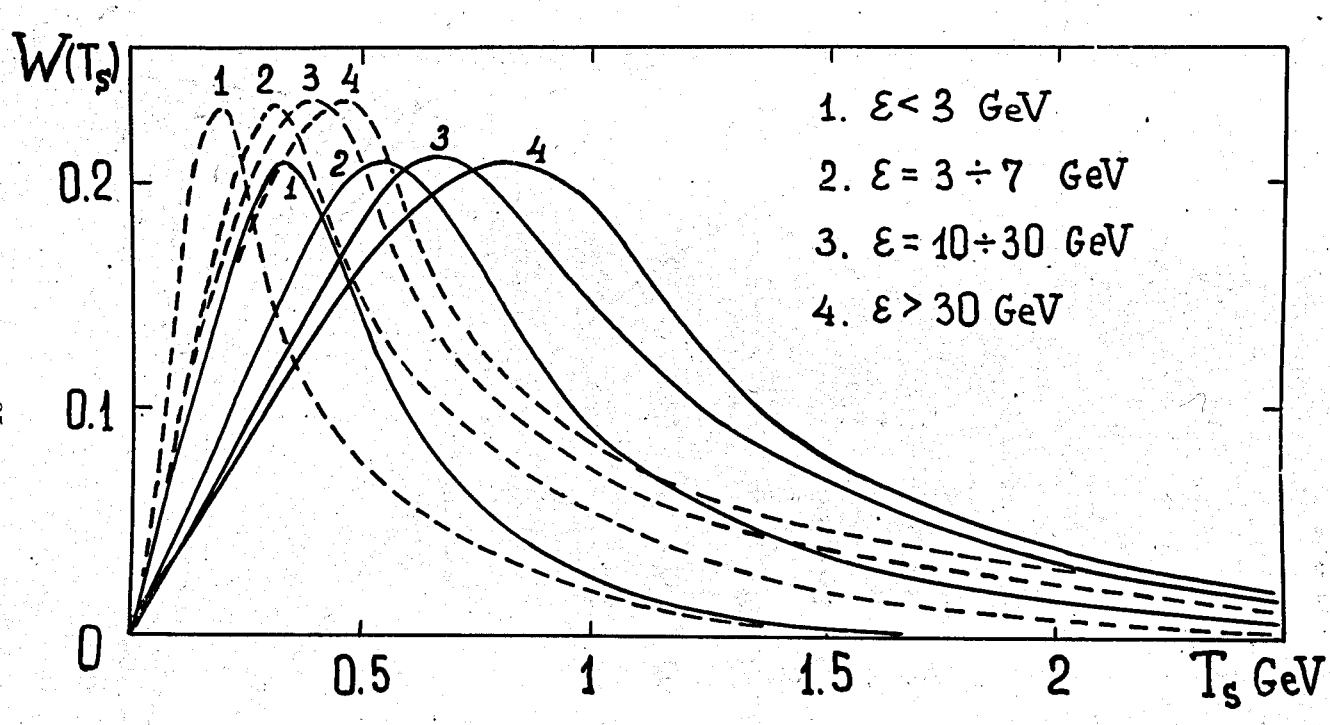

Fig.12. Energy distribution of pions (dashed line) and heavy particles (continuous lines) produced in inelastic MPI (in c.m.s.).

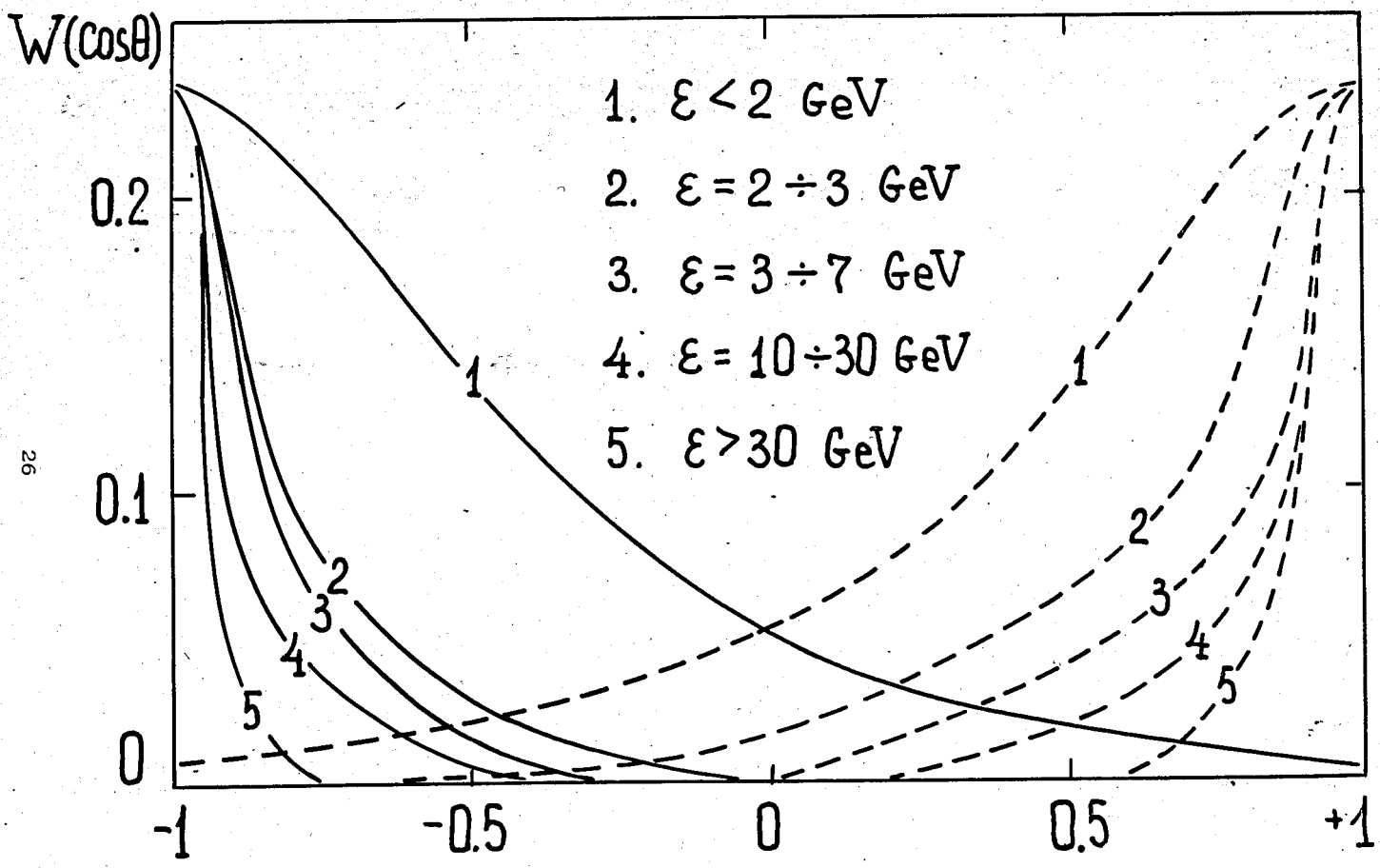

Fig.13. Angular distributions of particles produced in inelastic MPI —(in c.m.s.). All the notations are the same as in Fig.12.

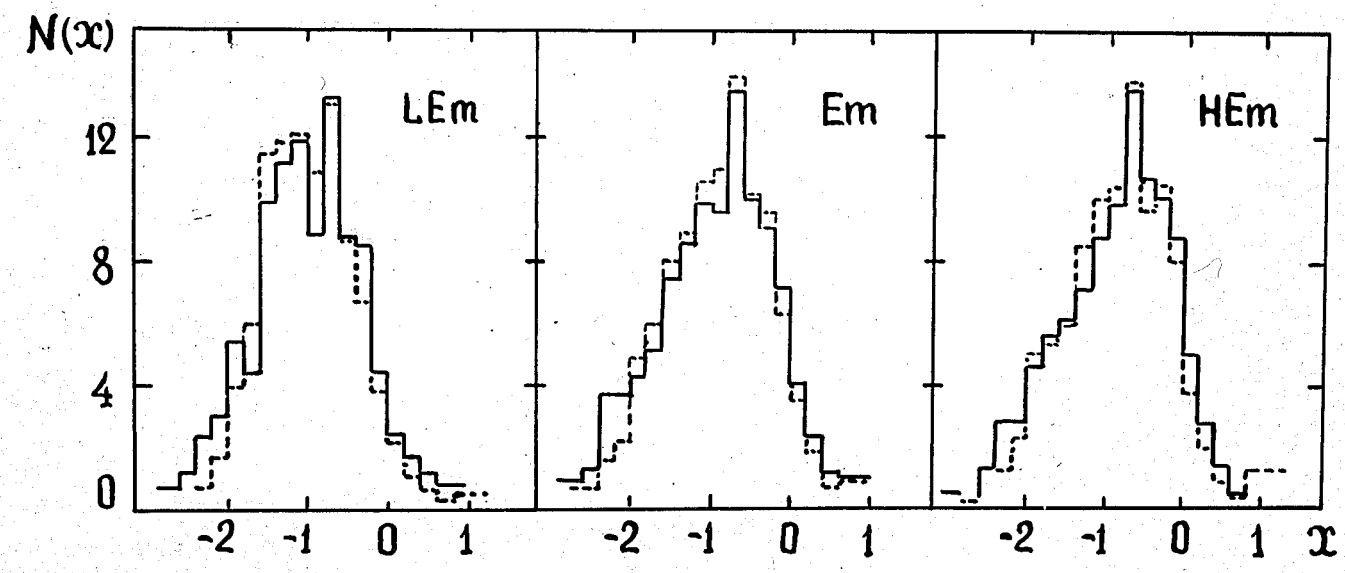

Fig.14. $x = \ell g\, tg\, \theta$ distribution of s -particles in emulsion stars produced by π^- mesons at an energy $T \approx 200$ GeV. The continuous histograms are the experiment of Gierula; the dashed lines are the caclulation results for $T = 200$ GeV.